Ecology, 100(10), 2019, e02798

Kelp beds and their local effects on seawater chemistry, productivity, and microbial communities

Catherine A. Pfister,[1,2,4] Mark A. Altabet,[3] and Brooke L. Weigel[2]

[1]*Department of Ecology and Evolution, University of Chicago, Chicago, Illinois 60637 USA*
[2]*Committee on Evolutionary Biology, University of Chicago, Chicago, Illinois 60637 USA*
[3]*School of Marine Sciences, University of Massachusetts, Dartmouth, Massachusetts 02744 USA*

Citation: Pfister, C. A., M. A. Altabet, and B. L. Weigel. 2019. Kelp beds and their local effects on seawater chemistry, productivity, and microbial communities. Ecology 100(10):e02798. 10.1002/ecy.2798

Abstract. Kelp forests are known as key habitats for species diversity and macroalgal productivity; however, we know little about how these biogenic habitats interact with seawater chemistry and phototroph productivity in the water column. We examined kelp forest functions at three locales along the Olympic Peninsula of Washington state by quantifying carbonate chemistry, nutrient concentrations, phytoplankton productivity, and seawater microbial communities inside and outside of kelp beds dominated by the canopy kelp species *Nereocystis luetkeana* and *Macrocystis pyrifera*. Kelp beds locally increased the pH, oxygen, and aragonite saturation state of the seawater, but lowered seawater inorganic carbon content and total alkalinity. Although kelp beds depleted nitrate and phosphorus concentrations, ammonium and dissolved organic carbon (DOC) concentrations were enhanced. Kelp beds also decreased chlorophyll concentrations and carbon fixed by phytoplankton, although kelp carbon fixation more than compensated for any difference in phytoplankton production. Kelp beds entrained distinct microbial communities, with higher taxonomic and phylogenetic diversity compared to seawater outside of the kelp bed. Kelp forests thus had significant effects on seawater chemistry, productivity and the microbial assemblages in their proximity. Thereby, the diversity of pathways for carbon and nitrogen cycling was also enhanced. Overall, these observations suggest that the contribution of kelp forests to nearshore carbon and nitrogen cycling is greater than previously documented.

Key words: blue carbon; carbon uptake; carbonate chemistry; climate change; Macrocystis pyrifera; Nereocystis luetkeana; *nutrient recycling; ocean acidification; primary productivity; seawater microbes.*

Introduction

Foundational species in ecosystems have primary roles in determining local diversity and multiple aspects of ecosystem function. Foundational primary producers support higher trophic levels, physically stabilize substrate, provide biogenic structure, and enhance species diversity (Dayton 1972). Although foundational species are typically found in high abundance, some have been compromised because of myriad anthropogenic stressors (Ellison et al. 2005). Canopy kelp are foundational species that form extensive underwater forests. They create critical habitat in temperate coastal environments worldwide, supporting animal productivity and diversity (Estes and Palmisano 1974, Bodkin 1986, Miller et al. 2018). Kelp species are also some of the fastest-growing primary producers (Mann 1973). For example, in the northeast Pacific, canopy kelp show linear growth rates of 12–14 cm per day (Graham et al. 2007), and can fix carbon at annual rates ranging from 0.2 to 14. 5 kg per square meter of benthos (Wheeler and Druehl 1986, North 1994). Kelp forest productivity also subsidizes filter-feeding animals (Duggins et al. 1989) and adjacent ecosystems, including the deep sea (Vetter and Dayton 1999, Krumhansl and Scheibling 2012). Although many kelp forests continue to have high-density populations (Pfister et al. 2018), others are documented to be in decline (Verges et al. 2014, Krumhansl et al. 2016). Because of the potential for kelp to take up and temporarily store large quantities of carbon (e.g., "blue carbon"; Duarte 2017), which would mitigate ocean-acidification–linked decreases in pH (Krause-Jensen and Duarte 2016), it is critical to assess their impact on seawater chemistry.

As significant primary producers, canopy kelp modifies the local seawater environment, creating physical gradients in carbon content, pH, alkalinity, and oxygen in seawater in their proximity (e.g., the giant kelp, *Macrocystis pyrifera*; Frieder et al. 2012, Koweek et al. 2017). These effects are sustained by the physical density of kelp, which inhibits water flow and mixing (Jackson and Winant 1983, Gaylord et al. 2007, Rosman et al. 2007). There is

Manuscript received 30 January 2019; revised 11 April 2019; accepted 28 May 2019. Corresponding Editor: Michael H. Graham.
[4] E-mail: cpfister@uchicago.edu

also potential for kelp to sequester large quantities of inorganic carbon during its growing season, which can locally mitigate pH declines associated with ocean acidification (e.g., Krause-Jensen and Duarte 2016) and enhance the growth of and development of calcifying species (e.g., Wahl et al. 2018, Hoshijima and Hofmann 2019). For kelp to fulfill this role as blue carbon, it is critical to understand to what extent kelp forests affect the seawater chemistry and productivity in their proximity.

Likely feedbacks between seawater chemistry and canopy kelp may be an additional mechanism through which canopy kelp affect the presence of other species. The high productivity of canopy kelp results in high levels of carbon fixation and could deplete resources such as nitrogen and phosphorus for other phototrophs or microbial chemolithotrophs. Canopy kelp also shade the water column. Phytoplankton have been suggested to compete with kelp for nutrients and light (Kavanaugh et al. 2009), and another study in California giant kelp beds suggests that production by canopy kelp, understory kelp, and phytoplankton are compensatory, and the summed productivity in the water column is relatively constant regardless of which phototrophs are dominant (Miller et al. 2011).

Canopy kelp may also enhance the opportunity for diverse microbial metabolisms, further increasing productivity by recycling carbon and nitrogen within the kelp forest. The vast surface area of canopy kelp provides substantial habitat for microbial populations, and the dissolved organic carbon (DOC) excreted by kelp (e.g., Reed et al. 2015) is a potential resource to microbial communities. Nearshore areas are known to have enhanced nitrogen cycling, based on inferences from stable nitrogen isotope analyses (Pfister et al. 2014*a*). Microbial nitrogen transformations were increased in association with a red alga (Pfister and Altabet 2019), and kelps host a diversity of microbial taxa (Bengtsson et al. 2010, Michelou et al. 2013, Lemay et al. 2018, Weigel and Pfister 2019). Larger kelp beds host greater bacterial abundances, including more alginate-lysate–producing bacteria (Clasen and Shurin 2015). Finally, as a potential locus for animal populations and microbial activity, kelp beds could be areas of rapid nutrient regeneration and recycling, enhancing multiple modes of carbon fixation.

We quantified the effects of kelp beds in the northeast Pacific Ocean on seawater chemistry, water column productivity, and the diversity of microbial assemblages. By repetitively sampling inside and outside of kelp beds over three sites, we were able to ascribe changes in these parameters due to the presence of the two co-occurring canopy-forming kelps, bull kelp (*Nereocystis luetkeana*) and the giant kelp (*Macrocystis pyrifera*).

Methods

Study site and sampling design

To test the effects of kelp beds on water column processes, we repeatedly sampled inside and outside of kelp beds as simultaneously as possible and over multiple days and sites. We sampled three locales that spanned the outer coast area of Washington state into the Straits of Juan de Fuca (Fig. 1). The westernmost locale and the one with the greatest exposure to open ocean conditions was Tatoosh Island (48.393689, −124.733820). East of Tatoosh and 7.1 km inside the Strait of Juan de Fuca is Koitlah Point (48.389408, −124.635702), and an additional 8.8 km eastward is Bullman Beach (48.356791, −124.535930). All three sites have high-density kelp beds first documented over 100 yr ago and persisting over the past 26 yr (index sites 16.3, 16.2, and 15.3, respectively; Pfister et al. 2018). At Tatoosh, we sampled within a *Nereocystis* canopy that has averaged 5.8 ha in extent since 1989, based on Washington Department of Natural Resources aerial surveys reported in Pfister et al. (2018). The Koitlah and Bullman sites have mixed assemblages of both *Nereocystis* and *Macrocystis*. The kelp bed surrounding Koitlah has averaged 103.5 ha in extent, and the Bullman bed has been at 73.5 ha since 1989. Both have had an approximate equal share of *Nereocystis* and *Macrocystis*, and sampling took place in both single- and mixed-species beds (Appendix S1: Table S1).

Paired collections were made inside and outside of the kelp bed from small boats that could navigate through dense kelp beds. While collecting water samples inside of the kelp bed, we took the mean of instrumental readings (see below) that logged every 30 s for 15 to 60 min to constitute a single sample. We then moved 200–400 m outside of the bed and repeated the procedure. On each day of sampling, we attempted to get at least three paired samples, depending upon weather and sea conditions. In this way, we censused 26 paired samples at Tatoosh Island, 19 at Koitlah Point, and 23 at Bullman Beach, with several samples that were unpaired. All were at the surface (1-m depth), during daylight hours, and over 27 sampling days in July and August of 2016 and 2017 (Appendix S1: Table S1), encompassing a range of oceanic and atmospheric conditions.

While sampling seawater for macronutrients, carbonate chemistry, and productivity estimates (see

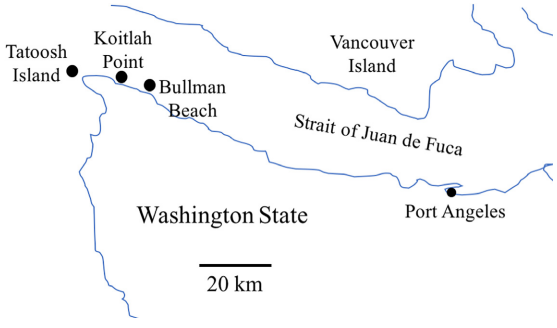

Fig. 1. A map of the study areas in the state of Washington, including Tatoosh Island, Koitlah Point, and Bullman Beach.

below), we also suspended an instrument (Hydrolab MS5 Sonde, Hach) to measure temperature, salinity, dissolved oxygen, chl *a*, and pH. The sonde was secured inside a PVC sleeve with a metal bracket with swivel bearings so it could rotate freely if necessary. In some instances, a sonde was temporarily moored inside the kelp bed with floatation and secured with kelp, while we tended an identical instrument outside the kelp bed. Additionally, on five separate occasions in 2018, we deployed the instrument overnight for up to 24 h at Bullman Beach; these five overnight deployments allowed us to quantify diel changes. GPS and water depth were always recorded. Although most of our seawater measurements were at 1-m water depth, we report seven replicate measures at depths to 6 m.

Light levels

Light was measured at each census date above the surface of the water using a LICOR LI-1000, with a LI-190 quantum sensor. Ambient light can be highly variable at these sites, because of time of day and the dynamics of clouds and fog, so a mean of multiple measures was often used. On several days we measured photosynthetically active radiation (PAR) throughout the water column with a LI-192 underwater sensor, both inside and outside the kelp bed. For subtidal measures, the sensor was attached to a PVC pole and lowered repeatedly down and up to a maximum depth of 6 m.

Measures of the seawater carbonate system

Total alkalinity (TA) and pH were measured from seawater collected by either submerging a 50-mL borosilicate glass bottle under the water surface and capping it with a glass ground stopper, or by overfilling the bottle from a tube attached to the Niskin sampler; care was taken so that the seawater minimally interacted with the atmosphere and air bubbles were absent. The samples were kept chilled and TA and pH were quantified within 48 h, though often within 6 h. For analysis, the samples were first incubated in a 25°C water bath. TA was measured with an Apollo SciTech AS-Alk2 SeaWATER gran titration with 0.1 N HCl. Spectrophotometric pH was analyzed with a Thermo-Fisher Genesys 10S UV-Vis spectrophotometer with a 1-cm cell width at wavelengths of 434, 578, and 730 nm, before and after one and then a second addition of 200 μL of c-Cresol Purple indicator solution was added (2 mmol). We calculated pH on the total scale using formulas in Dickson et al. (2007). Our TA and spectrophotometric measurements of pH were calibrated using a TA and pH standard from the Carbon Dioxide Quality Control Lab at Scripps Institute of Oceanography (TA: Batch 128, TA = 2,240.28 μmol/kg and Batch 165, TA = 2,214.09 μmol/kg at 25°C, pH: Batch 2, Bottle 82, pH = 8.092).

Aragonite saturation state, calcite saturation state, and pCO_2 were calculated with the "seacarb" package in R (Lavigne et al. 2011) using the spectrophotometric pH and TA measurements described above. Because we also measured phosphate, silica, and ammonium simultaneous with our carbonate collections, we tested if including these data improved estimation of our carbonate chemistry parameters. We found that including nutrient concentrations increased our estimate of aragonite saturation state, but only with an offset of 0.00033 units (n = 126 across all samples with nutrient, pH, and TA data). Our estimates of pCO_2 were similarly changed only a slight amount (−0.1768 ppm) when nutrient concentrations were included in the "seacarb" estimates. These nutrient effects on pCO_2 (only 0.02%) were less than our error in sampling these parameters in field conditions. We thus included nutrient measures in our carbonate system parameter measurements when we had them, but still estimated aragonite saturation state, calcite saturation state, and pCO_2 when nutrients were not measured.

To further characterize seawater chemistry in the kelp bed, we analyzed the isotopes of oxygen and carbon in seawater. The $\delta^{18}O$ of seawater was analyzed from seawater collected and stored in airtight 4-mL vials (borosilicate glass, screw cap with polyethylene cone liner) for later analysis at the University of Chicago (Olack et al. 2018). The isotopes of carbon in the dissolved inorganic carbon of seawater ($\delta^{13}C_{DIC}$) were determined from 1-mL seawater samples injected into 12-mL Exetainer tubes™ with phosphoric acid and evacuated with helium gas (Olack et al. 2018).

Measurements of particulate and dissolved organic matter and inorganic nutrients

Particulate organic matter concentration and isotopic composition in the seawater was measured by filtering 0.3–2.7 L of seawater through a Pall 47-mm filter holder (Pall Corporation, Port Washington, New York, USA) containing a Whatman GF/F 47-mm filter previously combusted at 350°C for 4 h. The amount of seawater filtered varied depending on the quantity of particulate matter in the water column. Filtering was done from a 2.5-L Niskin sampler (General Oceanics) or via hand-pumping (Guzzler™, Bosworth Co). The hand pump was necessary when sampling from a small Zodiac™ boat that had no structure for suspending the Niskin for gravity filtration. The filter was enclosed in a foil packet and dried at 60°C for 48 h. One-quarter of the filter was packed into a tin capsule (5 × 9 mm) prior to isotopic analysis. Samples were analyzed using a Costech 4010 Elemental Analyzer combustion system (Costech, Valencia, California, USA) coupled to a Thermo DeltaV Plus IRMS (Thermo Fisher Scientific, Waltham, MA, USA) via a Thermo Conflo IV interface (at the University of Chicago). Isotope reproducibility was 0.11‰ for $\delta^{13}C$ and 0.17‰ for $\delta^{15}N$.

Simultaneously, water collected from the filtrate was used to estimate concentrations of dissolved organic carbon (DOC), ammonium, nitrate, nitrite, phosphorus, and silica, as well as ^{15}N natural abundance isotope levels of NH_4^+. DOC was measured from approximately 25 mL of seawater filtered into 40-mL glass, carbon-free vials and immediately frozen. DOC was measured at the University of Washington Marine Chemistry lab (all methods from UNESCO 1994). All nutrient concentrations were determined from seawater filtered into HDPE bottles, frozen and analyzed at the University of Washington Marine Chemistry lab (methods from UNESCO 1994). Seawater frozen in an additional set of HDPE bottles was used to measure seawater $\delta^{15}NH_4$ isotopes at University of Massachusetts, Dartmouth using methods reported previously (Pather et al. 2014, Pfister et al. 2014*a*, 2016). Briefly, nitrogen-stable isotopes of ammonium were measured according to a modified version of the NH_4 oxidation method detailed in Zhang et al. (2007). NH_4 is oxidized to nitrite using a hypobromite solution and then reduced to N_2O using a sodium azide–acetic acid reagent before analysis on an IRMS (isotope ratio mass spectrometer).

Chlorophyll

Chlorophyll *a* was measured in three ways: (1) by filtering seawater and extracting pigments in ethanol, (2) by collecting water in situ for nearly immediate analysis with a portable fluorometer, and (3) by instrumental measure in situ with a MS5 (Hach Co.). For method 1, we filtered 150 mL of seawater through a Whatman 23 mm GF/F filter, placed the filter in 1.5 mL of ethanol, and froze it at −20°C until analysis. The concentration of these extracted pigments was measured with a Turner Model 450 Fluorometer against a chlorophyll *a* standard (spinach or *Anacystis nidulans*, Sigma), based on methods by Webb et al. (1992). We further acidified the samples with 1 N HCl to estimate the amount of chl *a* that was phaeophytin. The second measure of chl *a* was fluorescence of freshly collected samples determined with a portable fluorometer (AquaFluor™, Turner) by collecting 10 mL seawater in black plastic vials. Fluorescence was measured within ~3 h of sample collection. Each 10-mL sample yield 2–3 replicate measures per vial, which reduced variability due to differing buoyancy of the constituent phytoplankton. Our third measure of chl *a* used the fluorometer onboard the sonde, calibrated with a solid standard adjusted to measurements of chl *a* of known concentrations.

Comparing kelp vs. phytoplankton productivity

We used our measures of chl *a* concentration to estimate carbon uptake by phytoplankton using a relationship for the carbon fixed per unit of chl *a* based on ^{14}C uptake dynamics in nearby Dabob Bay, Washington (Welschmeyer and Lorenzen 1984). We compared calculated phytoplankton total carbon uptake to published carbon uptake estimates for *Nereocystis* and *Macrocystis*, assuming a water column of 7-m depth, the average depth of our kelp forest censuses, over 1 sq m of area. The mean ratio of chlorophyll *a* concentrations to micrograms of carbon fixed (Chl:C) was 53.65 at 1 m, 64.02 at 3 m, and 42.16 at 6 m. We applied our 1-m chl *a* reading to the first 3 m of depth, our 3-m chl *a* readings to the next 3-m depth interval, and our 6-m reading to the last meter to encompass a 7-m water column depth, where kelp is generally the most dense. For kelp, we used published values of standing kelp carbon uptake and carbon biomass (North 1994).

Seawater microbial composition

We compared the microbes in the water column in the immediate vicinity of the kelp bed with those outside the kelp bed by filtering approximately 1–3 L of seawater through Sterivex™ filters (mean = 1.4 L). Seawater was collected by holding an acid-washed plastic bottle under the seawater surface. The seawater was placed on ice and filtered the same day using a peristaltic pump. Samples for microbial analysis were collected using the same paired collections inside and outside of the kelp bed at the same time as the seawater chemistry parameters were sampled. From Jun through August of 2017, we collected 11 paired samples at Tatoosh Island and 9 paired samples each at Koitlah and Bullman Beach. Due to the vagaries of weather and boat operations, there were also three single samples at Tatoosh, one at Koitlah, and two at Bullman (Appendix S1: Table S1). All Sterivex cartridges were frozen and sent to storage at −80°C at the University of Chicago prior to extraction.

We extracted DNA from the Sterivex cartridge using the Power Soil DNA Extraction Kit (Qiagen), following the methodology described in Jackrel et al. (2017). The PCR amplification protocol followed (Caporaso et al. 2012) for multiplexing 16S rRNA samples, with a modified forward primer (Parada et al. 2016) to reduce sequencing bias (Walters et al. 2016). The V4 variable region of the 16S rRNA gene was amplified with the use of bar-coded primers according to EarthMicrobiome Project standard protocols (Thompson et al. 2017). PCR products were sequenced using an Illumina MiSeq paired-end run at Argonne National Lab.

We analyzed microbial 16S rRNA sequence data with Qiime2 (www.qiime2.org, Caporaso et al. 2010), using the DADA2 methodology to classify sequences as ASVs or amplicon sequence variants (Callahan et al. 2016). Briefly, DADA2 eliminates chimeras and sequencing error prior to determining ASVs. We assigned taxonomy with the GreenGenes database (13_8), trimmed to the V4 region, and subsequently removed chloroplast and mitochondria reads. We eliminated sequences that were present 10 times or less and subsampled sequences to 11,000 reads. Within Qiime2, we used the "diversity core-metrics-phylogenetic" function to generate metrics

of alpha and beta diversity. We further visualized microbial diversity with "phyloseq" in R (www.r-project.org).

We tested whether the alpha diversity of microbes, including phylogenetic diversity, differed inside and outside of the kelp bed and among the three locales using only our paired samples. We analyzed beta diversity among all samples to test whether microbial composition differed among the three sites and in proximity to the kelp bed. To analyze beta diversity, we used PERMANOVA and visualized results with nonmetric multidimensional scaling (NMDS) plots based on a Bray–Curtis distance matrix. We identified taxa that differed among the three locales and inside and outside the kelp bed using the analysis of composition of microbes (ANCOM) in Qiime2 (Mandal et al. 2015). We further tested whether microbial communities were identifiable in terms of where they came from by using the machine learning algorithm, Random Forest Classifier in Qiime2 (Bokulich et al. 2018), with 1,000 "estimators" or trees, for either the three locales or inside vs. outside the kelp bed.

Statistical methods

We structured our sampling to be pairwise, such that along each transect, we sampled both inside and outside the kelp bed. Linear mixed-effects models then tested the fixed effect of kelp bed (inside vs. outside) or locale (Bullman, Koitlah or Tatoosh) with the random effect of sample pair. Thus, even though many environmental parameters were highly variable over the study duration, our paired design allowed us to detect consistent differences inside and outside the kelp bed and among locales. Because of the constraints of sample costs and logistics of small boat operations, not all types of samples were collected on each sampling date. Appendix S1: Table 1 provides a key to sampling frequency. All statistical analyses were done in R Studio (v 1.1.456).

Results

Environmental parameters

Sea surface temperature was slightly colder outside kelp beds compared with inside, with a mean difference of 0.24°C. Sea surface temperature declined to the west, as expected from stronger upwelling at the outer coast area. Kelp beds had an anticipated strong effect on photosynthetically active radiation (PAR). During the day, PAR ranged from 1.4 to 2098.0 μmol/s/m^2 above the sea surface, depending on sun angle, cloud cover, time of day, and the density of coastal fog. PAR attenuated more rapidly inside the kelp bed than outside. On average, only 33.3% of the surface PAR reached 1-m depth, compared with 53.9% outside the kelp bed. At 3-m depth, 26.5% of surface PAR was present outside the bed, while only 13.5% of surface PAR penetrated to 3 m inside the bed. Kelp beds increased the oxygen content of the seawater by an average 0.69 mg/L (Fig. 2a, Table 1), though the oxygen content varied greatly depending on time of day (Appendix S2: Fig. S1) and amount of sunlight. The $\delta^{18}O$ of seawater became more enriched outside the kelp bed and westerly toward Tatoosh (Fig. 2b, Table 1), and was likely related to increasing salinity westward from Bullman (31.40 ppt) to Tatoosh (32.89).

Water nutrient concentrations were also affected by the presence of the kelp bed. Although nitrate and phosphate were more depleted within the kelp bed than outside (Fig. 2, Table 1), ammonium was typically greater within the kelp bed. Silica showed no consistent pattern between the two areas (Fig. 2d). Nutrients associated with upwelling (nitrate, phosphate, and silica) all increased toward the outer coast site of Tatoosh Island. While there were no overall differences in $\delta^{15}N_{NH4}$ isotope values among the 3 locales, the $\delta^{15}N_{NH4}$ was greater inside the kelp bed (Fig. 2h, Table 1).

Kelp beds alter the local carbonate system

We found significant differences inside and outside the kelp bed for every aspect of the carbonate system that we measured. On average, pH was greater inside the kelp bed by 0.08 (7.81 vs. 7.73), and TA decreased by 6.4 units (Fig. 3, Table 2). The $\delta^{13}C_{DIC}$ of seawater was, on average, 0.22 per mil greater inside the kelp bed (0.29 per mil inside vs. 0.11 outside), likely reflecting greater carbon uptake of the lighter isotope by kelp, which enriches the remaining isotopic ratio of seawater in the kelp bed. The least enriched carbon isotope ratio was outside the kelp bed at Tatoosh, a result consistent with upwelling of deep nutrient-rich water (Fig. 3c, Table 2).

Our 24-h instrumental measures of pH showed strong diel variation, ranging from 0.17 to 0.35 pH units (Appendix S2: Fig. S1) and demonstrating strong biological influences in the kelp forest. These relatively large diel fluctuations in pH were closely associated with changes in oxygen (Appendix S2: Fig. S1). We also observed differences in carbonate system parameters among the three sites, with pCO_2 and TA increasing westerly, while pH decreased (Table 2). The statistical differences in pH by locale differed slightly with instrumental pH vs. spectrophotometric pH, likely because spectrophotometric readings are from a single seawater measure, whereas the instrumental measures were a mean of multiple readings at 30-s intervals.

Our estimates of parameters of the carbonate system indicated that pCO_2 and aragonite and calcite saturation state showed a wide range of values during our censusing (Fig. 3, Table 2), yet exhibited consistent differences between inside vs. outside the kelp bed. On average, aragonite and calcite saturation states were 0.20 and 0.30 units greater inside the bed, respectively. Over multiple dates, the aragonite saturation state was below 1.0, and the calcite saturation state was typically below 3.0. The partial pressure of CO_2 (as pCO_2) was 167 μatm

TABLE 1. Environmental and macronutrient parameters measured inside and outside the kelp bed at three locales in Washington state. Linear mixed effects model with inside vs. outside and locale as fixed effects, and sampling pair as a random effect, including the number of complete pairs we had for each analysis. The *F* value and significance of each fixed effect is shown based on an analysis of variance on model results.

Response variable	Inside vs. outside of kelp bed	Inside vs. outside mean difference	Locale	Interaction	Number of paired samples
Sea surface Temperature (°C)	Inside > outside $F_{1,59} = 13.88$**	0.24	Decreases westerly $F_{2,67} = 23.02$**	$F_{2,59} = 2.796^{\S}$	62
Dissolved oxygen (mg/L)	Inside > outside $F_{1,57} = 20.90$**	0.69	Lower at Tatoosh $F_{2,66} = 2.94$**	Greatest difference at Tatoosh $F_{2,57} = 8.51$**	60
$\delta^{18}O$ of seawater	Inside < outside $F_{1,10} = 11.18$*	0.08	Increases westerly $F_{2,13} = 13.17$**	Greatest difference at Tatoosh $F_{2,10} = 9.01$*	13
[NH_4] in µM	Inside > outside $F_{1,50} = 6.42$*	0.29	$F_{2,57} = 0.72$	$F_{2,50} = 1.95$	53
[NO_3] in µM	Inside < outside $F_{1,50} = 32.53$**	2.29	Increases westerly $F_{2,57} = 10.44$**	$F_{2,50} = 4.74$*	53
[NO_2] in µM	Inside < outside $F_{1,50} = 15.09$**	0.02	$F_{2,57} = 0.89$	Greatest difference at Tatoosh $F_{2,57} = 6.97$*	53
[PO_4] in µM	Inside < outside $F_{1,50} = 4.82$*	0.05	Increases westerly $F_{2,57} = 12.35$**	Greatest difference at Tatoosh $F_{2,57} = 3.71$*	53
[Si] in µM	$F_{1,50} = 2.51$	NA	Increases westerly $F_{2,57} = 7.17$*	$F_{2,57} = 0.89$	53
$\delta^{15}N_{NH4}$ of seawater	Inside > outside $F_{1,16} = 14.69$*	2.81	$F_{2,19} = 0.094$	$F_{2,16} = 1.910$	19

Notes: *$0.001 < P < 0.05$, **$P < 0.001$, $^{\S}0.05 < P < 0.10$. Where inside and outside significantly differed, the mean difference is given.

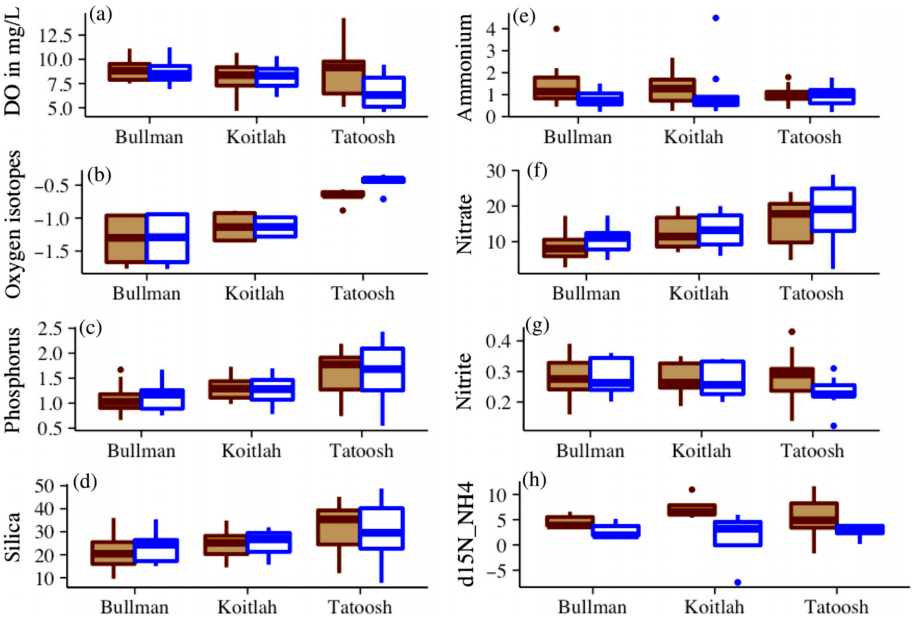

FIG. 2. Environmental variables and macronutrients measured at three sites as well as inside and outside the kelp bed. The filled brown box plots represent inside the kelp bed, and the open blue box plots are outside the kelp bed. All statistics are in Table 1 and are based on a linear mixed-effects model testing the fixed effects of site, kelp bed location, and their interaction, with sampling pair as a random effect. Nutrient concentrations are in µM. Box plots show the median as a horizontal line; 50% of all samples fall within the box and the upper and lower quartiles are shown with a vertical line.

lower inside the kelp bed when estimated with pH and TA values using "seacarb," but did not differ when we attempted to measure it directly (Olack et al. 2018), possibly because of the lower sample size for our direct measurement of DIC ($n = 32$) compared with twice the number of instrumental measures ($n = 64$).

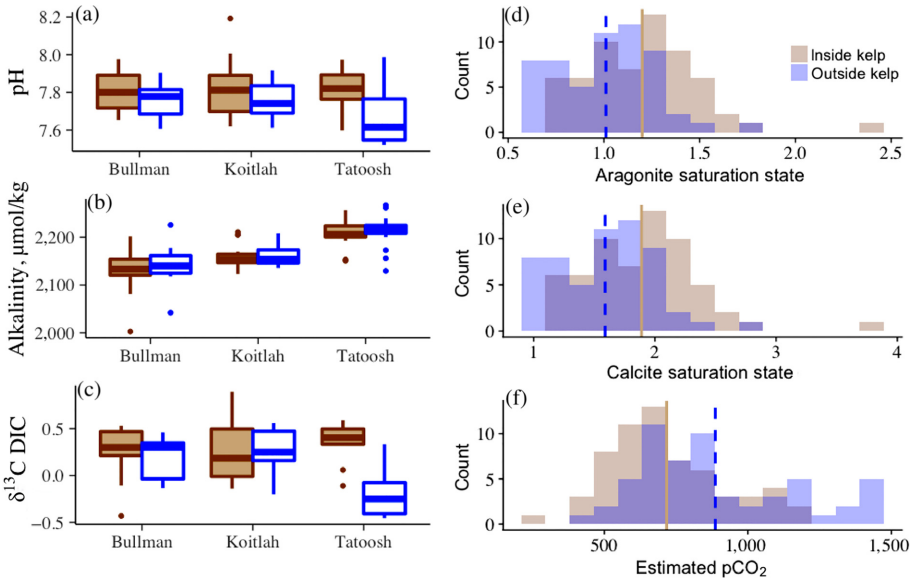

FIG. 3. Carbonate parameters measured inside and outside the kelp bed, including (a) pH, (b) total alkalinity (µmol/kg) and (c) $\delta^{13}C$ of dissolved inorganic carbon (DIC). Presentation as in Fig. 2. The distribution of carbonate parameters that were estimated (using seacarb in R) from all TA and pH measures included (d) aragonite saturation state, (e) calcite saturation state, and (f) the pCO_2 in seawater (in ppm). Vertical lines represent the mean for inside (solid line) and outside (dotted line) the kelp bed.

TABLE 2. Carbonate system parameters measured inside and outside the kelp bed at three locales in Washington state. From daytime pH and total alkalinity (TA) measures, we calculated daytime saturation states and pCO_2. Linear mixed effects model with inside vs. outside and locale as fixed effects, and transect pair as a random effect. The significance of each fixed effect is shown; key as in Table 1.

Response variable	Inside or outside of kelp bed	Inside vs. outside mean difference	Locale	Interaction	Number of paired samples
Spectrophotometric pH	Inside > outside $F_{1,55} = 50.40$**	0.087	$F_{2,65} = 1.00$	Greatest difference at Tatoosh $F_{1,55} = 8.70$*	68
Instrumental pH	Inside > outside $F_{1,49} = 3.60^{\S}$	0.024	Decreases westerly $F_{1,58} = 11.60$**	Greatest difference at Tatoosh $F_{1,49} = 6.10$*	52
Total alkalinity (µmol/kg)	Inside < outside $F_{1,51} = 5.70$*	6.39	Increases westerly $F_{1,61} = 37.50$**	$F_{1,51} = 0.20$	54
Dissolved inorganic carbon (mM)	$F_{1,24} = 0.025$	NA	$F_{2,29} = 2.38$	$F_{2,24} = 1.65$	27
$\delta^{13}C_{DIC}$	Inside > outside $F_{1,24} = 22.23$**	0.216	$F_{2,29} = 0.48$	Greatest difference at Tatoosh $F_{2,24} = 13.92$**	27
Aragonite saturation state	Inside > outside $F_{1,51} = 27.64$**	0.195	$F_{2,61} = 1.23$	$F_{2,51} = 1.98$	54
Calcite saturation state	Inside > outside $F_{1,51} = 27.64$**	0.307	$F_{2,61} = 1.25$	$F_{2,51} = 1.99$	54
pCO_2 (µatm)	Inside < outside $F_{1,51} = 34.22$**	167.1	Increases westerly $F_{2,61} = 3.12$*	Greatest difference at Tatoosh $F_{2,51} = 7.84$*	54

Notes: *$0.001 < P < 0.05$, **$P < 0.001$, $^{\S}0.05 < P < 0.10$. Where inside and outside significantly differed, the mean difference is given.

Kelp bed and water column productivity

Chlorophyll *a* was highly variable, ranging from almost undetectable to 15.2 µg/L during blooms. Water column chlorophyll (as chl *a* extracted with EtOH), declined significantly westward toward Tatoosh and increased by 50% outside kelp beds compared with inside (2.74 vs. 4.02, Fig. 4, Table 3). The estimates of chl *a* from ethanol-extracted samples were nearly identical whether or not the sample was acidified (regression slope = 1.04), indicating that phaeophytin was a relatively minor component and averaged only 5.4% of all extracted pigment concentrations. Phytoplankton *in vivo* fluorescence showed patterns similar to the extracted chl

a results, though the difference between inside and outside the kelp bed was only apparent at Tatoosh. Although we measured chl *a* with a fluorometer on the MiniSonde5, the instrumental in situ chl *a* measurements consistently deviated from extracted chlorophyll measures; samples inside the kelp bed were 25% higher than corresponding measurements outside the bed, likely due to interference of the fluorometry in the dense kelp canopy.

Although chl *a* was greater outside the kelp bed, particulate organic matter (POM) concentrations did not differ inside vs. outside (Fig. 4e, Table 3), suggesting that non-chlorophyll containing particulate organics were more abundant inside the kelp bed. Because chl *a* was only slightly greater outside the kelp bed, the chl a : POM ratio showed no significant difference. Chl *a* declined from 1- to 3–6-m depth, though the decline did not differ inside vs. outside the kelp bed (ANOVA, Depth * site interaction $F_{1,129} = 1.35$, $P = 0.247$). At 6-m depth, the decrease in chl *a* concentration was relatively comparable inside vs. outside the kelp bed.

As expected, DOC concentrations were higher inside the kelp bed, with a mean of 1.50 mg C/L (124.80 μM) inside compared to 1.02 mg C/L (84.53 μM) outside the bed, a 47% increase in DOC concentration inside the kelp bed (Fig. 4c, Table 3).

Seawater $\delta^{13}C_{DIC}$ was greater inside kelp beds, as was $\delta^{15}N$ of POM, whereas $\delta^{13}C$ of POM did not differ inside vs. outside the kelp bed. Across sites, the $\delta^{13}C$ of POM at Bullman was slightly more enriched compared to the other two sites (Fig. 4, Table 3).

Estimated total phytoplankton carbon uptake based on ratios of carbon : Chl *a* displayed a distribution of carbon uptake estimates, but mean carbon uptake per m^3 per day was higher outside the kelp bed (1.39 g) than inside (0.82 g; Fig. 4d).

Microbes inside and outside the kelp bed

Among the seawater samples that were analyzed for 16S rRNA ($n = 66$), there was a mean number of 28,949 sequences (range: 1,426–54,361). Three samples with fewer than 11,000 sequences were excluded from most analyses. ASV richness per sample, Faith's phylogenetic diversity, and the Shannon diversity index were all greater inside the kelp bed and highest within the kelp bed at Tatoosh Island (Figs. 5a–c, Table 3). Across all three locales, mean ASV diversity was 27.2% higher inside the kelp bed (299 vs. 235, $n = 29$ paired samples). The number of microbial taxa increased westerly along the Strait of Juan de Fuca, up to a maximum of 358 ASVs per sample at Tatoosh (Table 3). The increased diversity at Tatoosh was conspicuous at every sampling date and was evident even at the taxonomic level of bacterial order (Fig. 6). There was no difference in the total number of sequences per sample among the six spatial areas defined by three locales and inside vs. outside the kelp bed ($F_{5,57} = 0.439$, $P = 0.820$); thus, there was no site-to-site difference in our ability to detect diversity.

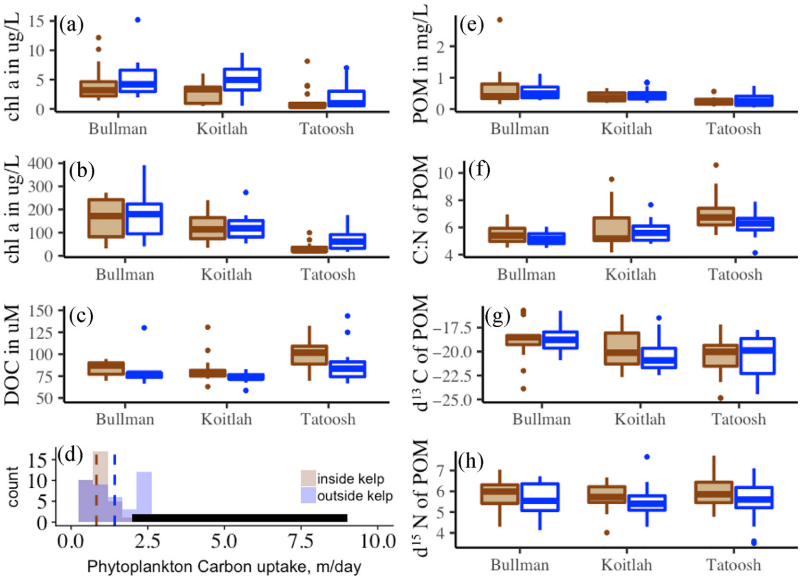

FIG. 4. The measurements of chlorophyll *a* and particulate organic matter (POM) inside and outside the kelp bed at three sites. Chlorophyll *a* measurements in micrograms per liter with (a) extracted chl *a*, (b) in vivo measurements of chl *a*, (c) the dissolved organic content (DOC) in micromoles. In (d), the estimates of carbon uptake solely by phytoplankton compared with the horizontal black line for all estimates of kelp carbon uptake in an equivalent volume of coastal water. The POM concentration (e) its C:N ratio (f) and the carbon (g) and nitrogen (h) isotopes of POM.

TABLE 3. Kelp bed effects on biological parameters measured inside and outside the kelp bed at three locales in Washington state. Linear mixed effects model with inside vs. outside and locale as fixed effects, and transect pair as a random effect. The significance of each fixed effect is shown.

Response variable	Inside or outside of kelp bed	Inside vs. outside mean difference	Locale	Interaction	Number of paired samples
Extracted chl *a*	Inside < outside $F_{1,45} = 26.59$**	1.28	Increases westerly $F_{1,53} = 16.87$**	$F_{1,45} = 1.77$	48
In vivo chl *a*	Inside < outside $F_{1,54} = 12.63$**	11.50	Increases westerly $F_{2,62} = 39.70$**	Effect greatest at Tatoosh $F_{1,54} = 7.67$*	57
POM (mg/L)	$F_{1,42} = 0.01$	NA	Decreases westerly $F_{2,49} = 10.13$**	$F_{1,42} = 0.93$	45
Dissolved organic carbon (mg/L)	Inside > outside $F_{1,44} = 21.22$**	0.54	Increases westerly $F_{2,49} = 7.53$*	Effect greatest at Tatoosh $F_{2,44} = 4.64$*	47
Chl *a* : POM	Inside < outside $F_{1,40} = 4.39$*	0.016	$F_{2,47} = 0.46$	$F_{2,40} = 0.93$	43
C:N ratio of particulate organic matter (POM)	Inside > outside $F_{1,40} = 9.26$*	0.387	Increases westerly $F_{2,49} = 8.26$**	$F_{2,40} = 1.06$	43
δ^{13}C of POM	$F_{1,43} = 0.97$	NA	Easterly site highest $F_{2,50} = 3.57$*	$F_{2,43} = 0.64$	47
δ^{15}N of POM	Inside > outside $F_{1,43} = 4.69$*	0.275	$F_{2,50} = 0.44$	$F_{2,43} = 0.21$	47
Carbon uptake by phytoplankton	Inside < outside $F_{1,47} = 18.39$**	0.56	Decreases westerly $F_{2,53} = 9.47$**	$F_{2,43} = 1.25$	50
Microbial amplicon sequence variants richness	Inside > outside $F_{1,55} = 13.057$**	67.5	Increases westerly $F_{2,55} = 5.446$*	$F_{2,55} = 1.012$	58
Microbial Faith's phylogenetic diversity	Inside > outside $F_{1,55} = 13.124$**	5.35	Increases westerly $F_{2,55} = 6.079$*	$F_{2,55} = 0.654$	58
Microbial Shannon diversity	Inside > outside $F_{1,55} = 6.616$*	0.35	Increases westerly $F_{2,55} = 4.979$*	$F_{2,55} = 0.151$	58
Microbial beta diversity (PERMANOVA)	$F_{1,59} = 3.379$*	NA	$F_{2,59} = 6.963$**	$F_{2,59} = 1.404$	62

Notes: *$0.001 < P < 0.05$, **$P < 0.001$, §$0.05 < P < 0.10$. Where inside and outside significantly differed, the mean difference is given.

An analysis of beta diversity indicated significant differences in microbial community composition among the three locales (PERMANOVA, pseudo-$F = 6.96$, $P < 0.001$) and inside vs. outside the kelp bed using all the samples (pseudo-$F = 3.38$, $P = 0.005$, Table 3, Fig. 5d). The beta diversity results were unchanged when we used alternate pairwise distance metrics to Bray–Curtis. Further evidence that there was a strong association between kelp beds and microbial communities resulted from the finding that seawater microbes were identifiable according to site and inside vs. outside the bed with a machine learning algorithm (Random Forest Classifier). Microbial taxa were assigned accurately to one of three locales 69.2% of the time and the algorithm predicted whether microbes were found inside vs. outside the kelp bed with 92.3% accuracy, indicating a strong association between kelp beds and their bacterioplankton communities. Although Tatoosh seawater always harbored the greatest taxonomic diversity, ANCOM revealed that there were also taxa enriched at Bullman and Koitlah (Appendix S3: Table S1). There were nine microbial taxa enriched inside of the kelp bed across all three sites (Appendix S3: Table S2), including ASVs from the phyla Bacteroidetes (family Flavobacteriaceae), Proteobacteria (families Rhodobacteraceae and Hyphomonadaceae and genera *Octadecabacter* and *Loktenella*), and Verrucomicrobia (genera *Persicirhabdus* and *Rubritalea*). All nine of these kelp bed-enriched taxa were also found on *Nereocystis* or *Macrocystis* blades from at least two sites (Appendix S3: Table S2), based on kelp surface microbial assemblages reported in Weigel and Pfister (2019). Two Alphaproteobacterial ASVs in the family Hyphomonadaceae family and the genus *Octadecabacter* had particularly high relative abundances on *Nereocystis* and *Macrocystis*.

DISCUSSION

Kelp forests effects on the seawater carbonate system

As has been found with an increasing number of studies of ocean macrophytes (Frieder et al. 2012, Hendriks et al. 2014, Krause-Jensen et al. 2015, Kapsenberg and Hofmann 2016, Krause-Jensen and Duarte 2016), our data indicate that the photosynthetic activities of kelp forests affect water column carbon dynamics by increasing pH, possibly favoring calcifying species. During the day, kelp forests increase pH and decrease total

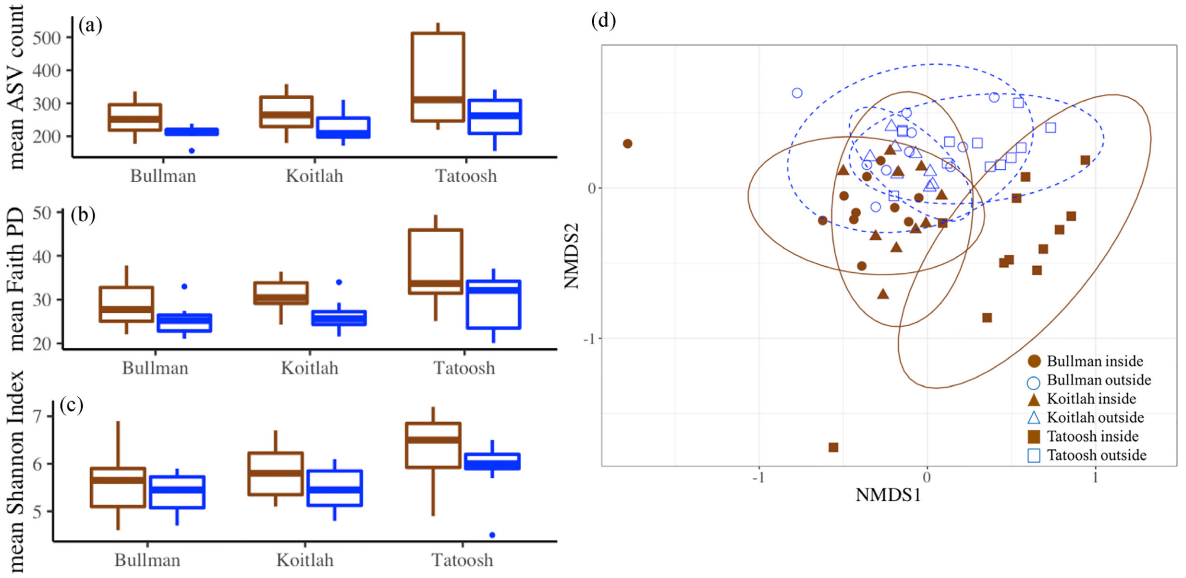

FIG. 5. Mean metrics of diversity for microbial data, including (a) the mean ASV count, (b) the mean Faith phylogenetic diversity index, and (c) the Shannon diversity index. All metrics were greater inside the kelp bed (brown) than outside (blue), and were greatest at Tatoosh Island (Table 3). The beta diversity in (d) using NMDS and based on a Bray–Curtis distance matrix, where filled circles are inside the kelp bed and empty circles are outside the bed. The three locales differed ($F_{2,59} = 6.963$, $P < 0.001$, PERMANOVA), and the microbial community was distinct inside vs. outside the kelp bed ($F_{1,59} = 3.379$, $P = 0.001$). The NMDS stress value was 0.157.

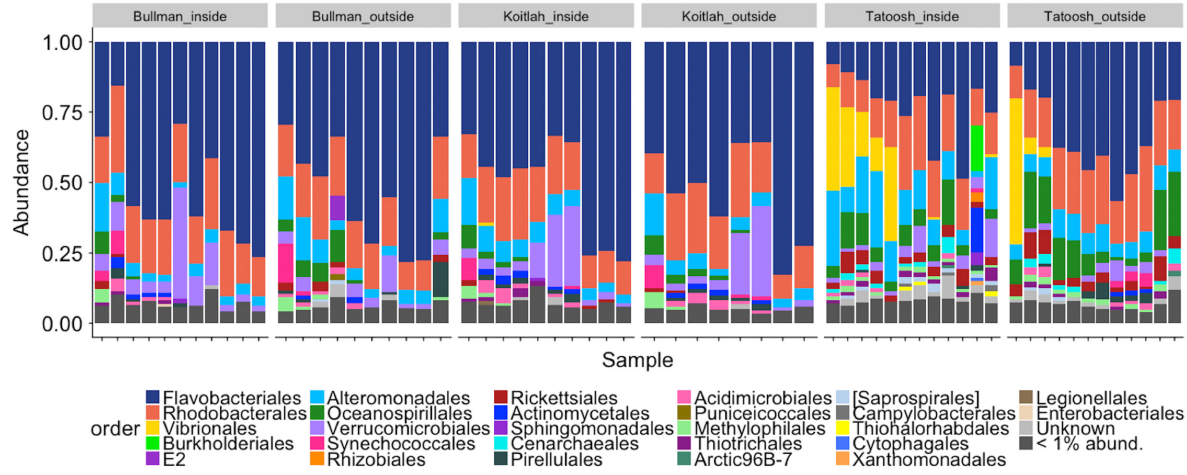

FIG. 6. The relative abundance of microbes within 27 orders for each of three sites, both inside and outside the kelp bed. Beyond the order-level differences, the ASV diversity was greatest inside of kelp beds and at Tatoosh overall (Table 3), and there were distinctions in ASVs among the three sites and inside vs. outside the bed (Appendix S3: Table S1).

alkalinity and pCO_2 (Fig. 3). A decrease in pH and pCO_2 was expected in the vicinity as these huge phototrophs removed pCO_2 from seawater. The decrease in alkalinity may be due to an increase in calcification within kelp beds or the metabolic activities of the kelp decreasing total alkalinity (e.g., Stepien et al. 2016). Estimated aragonite and calcite saturation states increased inside kelp beds, though the variance in those values was high. There were multiple time periods where aragonite was undersaturated (<1.0), which has also been demonstrated in a long-term Tatoosh Island time series (Wootton and Pfister 2012). Previous controlled studies show that aragonite and calcite saturation state of seawater increased with macrophytes (Stepien et al. 2016), further supporting our observations that pH fluctuations vary with kelp photosynthesis.

Kelp and other coastal macrophytes have been proposed as important blue carbon sinks for their potential

to take up carbon and locally ameliorate declining pH (Duarte 2017). During 2016 and 2017, there were 1,510.7 and 1,355.4 hectares of canopy kelp forests in Washington state, respectively (Pfister et al. 2018), generating an estimated range of 30.2 to 135.9 metric tons of C uptake per day in 2016 and 27.1 to 121.9 in 2017. Although this estimate for Washington, and estimates elsewhere (e.g., Wilmers et al. 2012), suggests that kelp beds can fix impressive amounts of carbon during the spring and summer growing season and during daylight hours, most studies do not consider the transient nature of this fixed carbon. First, nighttime measures in the kelp bed show that on some days, pH values at night were as much as 0.35 units lower than daytime values during the same 24-h period (Appendix S2: Fig. S1). Algal species respire in the absence of sunlight, resulting in respired CO_2 entering the surrounding water. Diel cycles in the coastal carbonate cycle have been documented (Yates et al. 2007, Wootton et al. 2008, Frieder et al. 2012) and are likely ubiquitous. Although there is release of sequestered carbon at night, we know relatively little about the fate of the remaining carbon fixed by kelp tissue. Through herbivory and wave disturbance, some carbon becomes particulate organic matter (Pessarrodona et al. 2018), and as much as 14–26% of fixed carbon is excreted as DOC (Abdullah and Fredriksen 2004, Reed et al. 2015), consistent with our finding of higher DOC within the kelp bed. Export of kelp biomass to deeper areas is also demonstrated (Krumhansl and Scheibling 2012, Filbee-Dexter and Scheibling 2014). Further, large rafts of kelp decompose in situ and in nearby coastal areas (Harrold and Lisin 1989), likely resulting in the respiration of carbon and its return to seawater and the atmosphere.

Although the kelp beds studied here decrease carbon locally and result in conditions conducive to calcification, this effect may be temporary and confined to daylight periods during the spring and summer growing season, the period of this study. Our research likely bracketed the period of time when kelp has a maximal effect on seawater chemistry, given that *Nereocystis* is an annual species and is nearly completely removed by fall and winter storms; the abundance of *Macrocystis* is also reduced during the fall and winter months. However, if calcifying animals take advantage of these pH cycles by timing their calcification to periods of high pH (e.g., Wahl et al. 2018), these diel and seasonal cycles could be significant.

Kelp forest effects on primary production

Canopy kelps are large phototrophs that reduce nitrate and phosphorus concentrations, as well as shade the water column (Fig. 2, Gerard 1982, Reed and Foster 1984), thereby potentially reducing the productivity of other phototrophs. Miller et al. (2011) found phytoplankton increased in concentration when *Macrocystis* was experimentally removed in California, though the response varied from halving the productivity of phytoplankton to having no detectable effect. In our study, although the kelp bed reduced chl *a* concentration at the surface (Fig. 4), the concentration of POM did not differ inside vs. outside the kelp bed (Fig. 4; see also Miller et al. 2011). Our own estimates for phytoplankton and published studies of *Macrocystis* and *Nereocystis* carbon fixation suggest that the 0.56-g greater total carbon fixed by phytoplankton outside of a kelp bed in a hypothetical 7-m water column (1 × 1 m) is relatively small compared with the additional 2.0–9.0 g C fixed in that same volume of water by canopy kelp (North 1994). When *Macrocystis* was removed in California, phytoplankton net primary production increased as much as 1.5–2 times, a multiplier similar to what we found inside vs. outside the kelp bed (Miller et al. 2011). Thus, although the presence of kelp decreased phytoplankton carbon fixation by 0.56 g C, the activity of canopy kelp is 3 to 15 times greater than the phytoplankton difference (Fig. 4), resulting in overall greater productivity in a kelp bed than areas without. Thus, there is not strict complementarity in productivity. Even if understory kelp are present when canopy kelp are not, they are unable to grow vertically through the water column to a higher light environment and thus will not provide the same biomass across a depth gradient. Whether the reverse is important, that phytoplankton productivity inhibits kelp canopy growth, is untested here, but phytoplankton abundance has been shown to be a negative correlate of low intertidal macrophyte abundance in Oregon (Kavanaugh et al. 2009).

Our estimates of carbon fixation included photosynthetic uptake by phytoplankton and kelp but do not include chemolithotrophic or mixotrophic microbial carbon use. The ability of microbes to utilize many alternative pathways for carbon fixation (Hügler and Sievert 2011) means that productivity estimates based on chl a pigment concentrations or kelp biomass will be an underestimate. Although we do not yet know the functional gene composition of the microbial taxa discovered here, the increased diversity of microbial ASVs inside the kelp bed suggests that the presence of kelp potentially increases metabolic opportunities for microbes, including enhanced carbon fixation, and is an area that deserves future investigation.

In addition to increased microbial diversity in kelp beds, kelp beds altered seawater chemistry in ways suggesting positive interactions via nutrient recycling, rather than strict competition for nutrients. Carbon is exuded as DOC from kelp tissues, elevating DOC concentrations within the kelp bed, thus providing an organic carbon resource for heterotrophic microbial processes (Kirchman 1994, Butturini and Sabater 2000). Previous studies with a red alga in this ecosystem, *Prionitis sternbergii*, suggested increased activity of microbes in association with the alga (e.g., Pfister et al. 2014*b*), which were further enhanced with the experimental addition of DOC (Pfister and Altabet 2019). The rich animal life

within a kelp bed (Harvell 1984, Bodkin 1986, Miller et al. 2018) is likely responsible for the increased ammonium that we documented inside kelp beds. As the most reduced form of inorganic nitrogen, ammonium is a preferred choice for phototrophs and an important energy source for chemolithotrophic microbes. The greater isotope value for $\delta^{15}N_{NH4}$ further suggests the importance of ammonium recycling within the kelp forest and the potential for nutrient regeneration.

The differences we have documented in chemical and biological parameters depend upon the flow around and within kelp beds, which is a highly variable process. The attenuation of flow both along and across a kelp bed (Jackson and Winant 1983, Gaylord et al. 2007, Rosman et al. 2007) suggests that local effects of kelp on the surrounding seawater can persist. We found that temperature was consistently higher inside kelp beds, a result shared with Hoshijima and Hofmann (2019), suggesting retention of seawater inside kelp beds. In our study, the differences in pH, carbon, and oxygen within and outside the bed were often the greatest at Tatoosh. The combination of strong currents around the island and the extension of a dense kelp bed into a north-facing cove may result in a strong local gradient in flow that is strengthened by the kelp bed at Tatoosh.

Kelp forests entrain distinct microbial communities

Seawater from within kelp beds harbored significantly distinct microbial assemblages at all sites, with the greatest taxonomic diversity inside of the kelp bed. Previous incubations of seawater with *Nereocystis* lasting 5 d in duration resulted in increased microbial diversity in the seawater (Chen and Parfrey 2018). Whether the enhanced microbial diversity within the kelp forest was due to kelp directly sloughing microbial taxa into the water column, or due to the provisioning of seawater microbial communities with metabolic resources (e.g., Nelson et al. 2013) is still unknown. The significant differences in carbon and nitrogen biogeochemistry that we measured inside vs. outside of the kelp bed coincided with the strongest microbial contrasts. A number of environmental variables showed an interaction between site and whether the sampling occurred in or outside of the kelp bed, and this interaction was always due to a greater difference between the inside and the outside of the bed at Tatoosh (Tables 1–3). All nine taxa that had a significantly greater relative abundance inside kelp beds were found on either *Nereocystis* or *Macrocystis* in a study of surface-associated microbes (Weigel and Pfister 2019). Kelp-bed–enriched taxa included Flavobacteriaceae, which are often hosted by *Macrocystis* (Michelou et al. 2013, Vollmers et al. 2017, Minich et al. 2018), are usually aerobic (McBride 2014), and were also an abundant component in the Monterey Bay, California kelp bed (Wilson et al. 2018). Microbes in association with *Macrocystis* were enriched in nitrogen metabolic functions compared to surrounding seawater (Minich et al. 2018), which may contribute to increased nitrogen recycling and the pattern of increased $^{15}N_{NH4}$ within the kelp bed.

If the microbial taxonomic diversity in association with kelp beds has corresponding functional and metabolic diversity, then the contribution of kelp forests to coastal nutrient dynamics is underestimated. The enhancement of taxonomic diversity inside the kelp bed may indicate that there are kelp-associated microbes that are capable of respiring or assimilating organic matter supplied by the kelp host (Lin et al. 2018). Other possible microbial metabolisms may include microbial production of vitamin B12 (Dogs et al. 2017), or the utilization of dissolved inorganic nitrogen (Minich et al. 2018). In sum, kelp forests have distinct effects on the biogeochemistry, the productivity, and the microbial diversity in the surrounding seawater. The microbial diversity in proximity to kelp (Minich et al. 2018, Weigel and Pfister 2019) make it likely that the biogeochemical effects that kelp forests have are due, in part, to associated microbial populations.

Conclusions

The presence of canopy kelp forests across the three study sites was associated with a suite of changes to water column chemistry, productivity, and microbial diversity. Foundational species that are also phototrophs, such as kelp, have the potential to change the local environment greatly through their effects as biogenic habitat and, as demonstrated here, through their effects on key processes such as carbon and nitrogen dynamics. Kelp beds altered local nutrient dynamics by increasing DOC and removing inorganic nutrients (NO_3, NO_2, PO_4), yet increases in NH_4 concentrations and enriched isotope values suggest that kelp beds promoted nitrogen regeneration. Kelp beds locally retain highly diverse microbial communities, which likely host diverse metabolisms and contribute to the biogeochemical effects that kelp forests have on the surrounding seawater. Although kelp beds are ubiquitous features in temperate oceans and have a documented presence at some sites for decades (Pfister et al. 2018, Carnell and Keough 2019), they are also in decline in many areas (Verges et al. 2014, Krumhansl et al. 2016). Thus, our documentation that kelp beds reduced seawater inorganic carbon content, while increasing pH, oxygen, and microbial diversity, suggests an important role for phototrophic foundational species in temperate marine systems and a need to maintain their function.

Acknowledgments

The NOAA-COCA program funded this research through NA16OAR431055 (CAP) and NA16OAR431056 (MAA). A Department of Education GAANN fellowship supported BLW. We thank the Olympic Coast National Marine Sanctuary, the Makah Tribal Nation, and the U.S. Coast Guard–Neah Bay for facilitating boat access to all sites; A. Friel, L. Antrim, and R.

Ross were expert skippers. H. Berry of the Washington Department of Natural Resources provided kelp bed expertise. A. Akmajian, L. Antrim, H. Berry, M. Bitter, T. Bowyer, O. Cattau, T. Chambers, A. Friel, K. Miranda, J. Scordino, J. Waddell, A. M. Wootton, J. B. Wootton, and J. T. Wootton all helped in the field. R. An, C. Sauceda, and M. Verner-Crist helped with lab analyses. K. Krogsland and A. Morello once again provided expertise at the University of Washington Marine Chemistry lab, and G. Olack and R. Roy provided isotope expertise and analysis. The J. Gilbert lab, especially S. Owens and N. Gottel, helped in all aspects of microbial genomics. J. T. Wootton, K. Silliman, M. Graham, and two anonymous reviewers improved an earlier version of the ms.

Literature Cited

Abdullah, M. I., and S. Fredriksen. 2004. Production, respiration and exudation of dissolved organic matter by the kelp *Laminaria hyperborea* along the west coast of Norway. Journal of the Marine Biological Association of the United Kingdom 84:887–894.

Bengtsson, M., K. Sjøtun, and L. Øvreås. 2010. Seasonal dynamics of bacterial biofilms on the kelp *Laminaria hyperborea*. Aquatic Microbial Ecology 60:71–83.

Bodkin, J. L. 1986. Fish assemblages in *Macrocystis* and *Nereocystis* kelp forests off Central California. Fishery Bulletin 84:799–808.

Bokulich, N. A., B. D. Kaehler, J. R. Rideout, M. Dillon, E. Bolyen, R. Knight, G. A. Huttley, and J. Gregory Caporaso. 2018. Optimizing taxonomic classification of marker-gene amplicon sequences with QIIME 2's q2-feature-classifier plugin. Microbiome 6:90.

Butturini, A., and F. Sabater. 2000. Seasonal variability of dissolved organic carbon in a Mediterranean stream. Biogeochemistry 51:303–321.

Callahan, B. J., P. J. McMurdie, M. J. Rosen, A. W. Han, A. J. A. Johnson, and S. P. Holmes. 2016. DADA2: high-resolution sample inference from Illumina amplicon data. Nature Methods 13:581–583.

Caporaso, J. G. et al. 2010. QIIME allows analysis of high-throughput community sequencing data. Nature Methods 7:335–336.

Caporaso, J. G. et al. 2012. Ultra-high-throughput microbial community analysis on the Illumina HiSeq and MiSeq platforms. The ISME Journal 6:1621–1624.

Carnell, P. E., and M. J. Keough. 2019. Reconstructing historical marine populations reveals major decline of a kelp forest ecosystem in Australia. Estuaries and Coasts 42:765–778.

Chen, M. Y., and L. W. Parfrey. 2018. Incubation with macroalgae induces large shifts in water column microbiota, but minor changes to the epibiota of co-occurring macroalgae. Molecular Ecology 27:1966–1979.

Clasen, J. L., and J. B. Shurin. 2015. Kelp forest size alters microbial community structure and function on Vancouver Island, Canada. Ecology 96:862–872.

Dayton, P. K. 1972. Toward an understanding of community resilience and the potential effects of enrichments to the benthos at McMurdo Sound, Antarctica. Pages 81–86 in B. C. Parker, editor, Proceedings of the Colloquium on Conservation Problems. Allen Press, Lawrence, Kansas, USA.

Dickson, A. G., C. L. Sabine, J. R. Christian, C. P. Bargeron, and North Pacific Marine Science Organization, editors. 2007. Guide to best practices for ocean CO2 measurements. North Pacific Marine Science Organization, Sidney, BC.

Dogs, M., B. Wemheuer, L. Wolter, N. Bergen, R. Daniel, M. Simon, and T. Brinkhoff. 2017. Rhodobacteraceae on the marine brown alga *Fucus spiralis* are abundant and show physiological adaptation to an epiphytic lifestyle. Systematic and Applied Microbiology 40:370–382.

Duarte, C. M. 2017. Reviews and syntheses: hidden forests, the role of vegetated coastal habitats in the ocean carbon budget. Biogeosciences 14:301–310.

Duggins, D. O., C. A. Simenstad, and J. A. Estes. 1989. Magnification of secondary production by kelp detritus in coastal marine ecosystems. Science 245:170–173.

Ellison, A. M., et al. 2005. Loss of foundation species: consequences for the structure and dynamics of forested ecosystems. Frontiers in Ecology and the Environment 3:479.

Estes, J. A., and J. F. Palmisano. 1974. Sea otters: their role in structuring nearshore communities. Science 185:1058–1060.

Filbee-Dexter, K., and R. Scheibling. 2014. Detrital kelp subsidy supports high reproductive condition of deep-living sea urchins in a sedimentary basin. Aquatic Biology 23:71–86.

Frieder, C. A., S. H. Nam, T. R. Martz, and L. A. Levin. 2012. High temporal and spatial variability of dissolved oxygen and pH in a nearshore California kelp forest. Biogeosciences 9:3917–3930.

Gaylord, B., et al. 2007. Spatial patterns of flow and their modification within and around a giant kelp forest. Limnology and Oceanography 52:1838–1852.

Gerard, V. A. 1982. In situ rates of nitrate uptake by giant kelp, *Macrocystis pyrifera* (L.) C. Agardh: tissue differences, environmental effects, and predictions of nitrogen-limited growth. Journal of Experimental Marine Biology and Ecology 62:211–224.

Graham, M., J. Vásquez, and A. Buschmann. 2007. Global ecology of the giant kelp *Macrocystis*: from ecotypes to ecosystems. Oceanography and Marine Biology: An Annual Review 45:39–88.

Harrold, C., and S. Lisin. 1989. Radio-tracking rafts of giant kelp: local production and regional transport. Journal of Experimental Marine Biology and Ecology 130:237–251.

Harvell, C. D. 1984. Predator-induced defense in a marine bryozoan. Science 224:1357–1359.

Hendriks, I. E., Y. S. Olsen, L. Ramajo, L. Basso, A. Steckbauer, T. S. Moore, J. Howard, and C. M. Duarte. 2014. Photosynthetic activity buffers ocean acidification in seagrass meadows. Biogeosciences 11:333–346.

Hoshijima, U., and G. E. Hofmann. 2019. Variability of seawater chemistry in a kelp forest environment is linked to in situ transgenerational effects in the purple sea urchin, *Strongylocentrotus purpuratus*. Frontiers in Marine Science https://doi.org/10.3389/fmars.2019.00062

Hügler, M., and S. M. Sievert. 2011. Beyond the Calvin cycle: autotrophic carbon fixation in the ocean. Annual Review of Marine Science 3:261–289.

Jackrel, S. L., S. M. Owens, J. A. Gilbert, and C. A. Pfister. 2017. Identifying the plant-associated microbiome across aquatic and terrestrial environments: the effects of amplification method on taxa discovery. Molecular Ecology Resources 17:931–942.

Jackson, G. A., and C. D. Winant. 1983. Effect of a kelp forest on coastal currents. Continental Shelf Research 2:75–80.

Kapsenberg, L., and G. E. Hofmann. 2016. Ocean pH time-series and drivers of variability along the northern Channel Islands, California, USA: temperate coastal ocean pH variability. Limnology and Oceanography 61:953–968.

Kavanaugh, M. T., K. J. Nielsen, F. T. Chan, B. A. Menge, R. M. Letelier, and L. M. Goodrich. 2009. Experimental assessment of the effects of shade on an intertidal kelp: Do phytoplankton blooms inhibit growth of open coast macroalgae? Limnology and Oceanography 54:276–288.

Kirchman, D. L. 1994. The uptake of inorganic nutrients by heterotrophic bacteria. Microbial Ecology 28:255–271.

Koweek, D. A., K. J. Nickols, P. R. Leary, S. Y. Litvin, T. W. Bell, T. Luthin, S. Lummis, D. A. Mucciarone, and R. B. Dunbar. 2017. A year in the life of a central California kelp forest: physical and biological insights into biogeochemical variability. Biogeosciences 14:31–44.

Krause-Jensen, D., and C. M. Duarte. 2016. Substantial role of macroalgae in marine carbon sequestration. Nature Geoscience 9:737–742.

Krause-Jensen, D., C. M. Duarte, I. E. Hendriks, L. Meire, M. E. Blicher, N. Marbà, and M. K. Sejr. 2015. Macroalgae contribute to nested mosaics of pH variability in a subarctic fjord. Biogeosciences 12:4895–4911.

Krumhansl, K. A. et al. 2016. Global patterns of kelp forest change over the past half-century. Proceedings of the National Academy of Sciences 113:13785–13790.

Krumhansl, K. and R. Scheibling. 2012. Production and fate of kelp detritus. Marine Ecology Progress Series 467:281–302.

Lavigne, H., J. Epitalon, and J.-P. Gattuso. 2011. seacarb: seawater carbonate chemistry with R. R package version 3.0. R Project. https://CRAN.R-project.org/package=seacarb

Lemay, M. A., P. T. Martone, P. J. Keeling, J. M. Burt, K. A. Krumhansl, R. D. Sanders, and L. Wegener Parfrey. 2018. Sympatric kelp species share a large portion of their surface bacterial communities: kelp-associated bacterial diversity. Environmental Microbiology 20:658–670.

Lin, J. D., M. A. Lemay, and L. W. Parfrey. 2018. Diverse bacteria utilize alginate within the microbiome of the giant kelp *Macrocystis pyrifera*. Frontiers in Microbiology https://doi.org/10.3389/fmicb.2018.01914

Mandal, S., W. Van Treuren, R. A. White, M. Eggesbø, R. Knight, and S. D. Peddada. 2015. Analysis of composition of microbiomes: a novel method for studying microbial composition. Microbial Ecology in Health and Disease 26:27663.

Mann, K. H. 1973. Seaweeds: their productivity and strategy for growth. Science 182:975–981.

McBride, M. J. 2014. The family Flavobacteriaceae. Pages 643–676 *in* E. Rosenberg, E. F. DeLong, S. Lory, E. Stackebrandt, and F. Thompson, editors. The prokaryotes: other major lineages of bacteria and the archaea. Springer, Berlin, Germany.

Michelou, V. K., J. G. Caporaso, R. Knight, and S. R. Palumbi. 2013. The Ecology of microbial communities associated with *Macrocystis pyrifera*. PLoS ONE 8:e67480.

Miller, R. J., K. D. Lafferty, T. Lamy, L. Kui, A. Rassweiler, and D. C. Reed. 2018. Giant kelp, *Macrocystis pyrifera*, increases faunal diversity through physical engineering. Proceedings of the Royal Society B 285:20172571.

Miller, R. J., D. C. Reed, and M. A. Brzezinski. 2011. Partitioning of primary production among giant kelp (*Macrocystis pyrifera*), understory macroalgae, and phytoplankton on a temperate reef. Limnology and Oceanography 56:119–132.

Minich, J. J., M. M. Morris, M. Brown, M. Doane, M. S. Edwards, T. P. Michael, and E. A. Dinsdale. 2018. Elevated temperature drives kelp microbiome dysbiosis, while elevated carbon dioxide induces water microbiome disruption. PLoS ONE 13:e0192772.

Nelson, C. E., S. J. Goldberg, L. Wegley Kelly, A. F. Haas, J. E. Smith, F. Rohwer, and C. A. Carlson. 2013. Coral and macroalgal exudates vary in neutral sugar composition and differentially enrich reef bacterioplankton lineages. The ISME Journal 7:962.

North, W. J. 1994. Review of *Macrocystis* biology. Pages 447–527 *in* I. Akatsuka, editor. Biology of economic algae. SPB Academic Publishing, The Hague, Netherlands.

Olack, G. A., A. S. Colman, C. A. Pfister, and J. T. Wootton. 2018. Seawater DIC analysis: the effects of blanks and long-term storage on measurements of concentration and stable isotope composition: the analysis of seawater carbon. Limnology and Oceanography: Methods 16:160–179.

Parada, A. E., D. M. Needham, and J. A. Fuhrman. 2016. Every base matters: assessing small subunit rRNA primers for marine microbiomes with mock communities, time series and global field samples: Primers for marine microbiome studies. Environmental Microbiology 18:1403–1414.

Pather, S., C. A. Pfister, D. M. Post, and M. A. Altabet. 2014. Ammonium cycling in the rocky intertidal: remineralization, removal, and retention. Limnology and Oceanography 59:361–372.

Pessarrodona, A., P. J. Moore, M. D. J. Sayer, and D. A. Smale. 2018. Carbon assimilation and transfer through kelp forests in the NE Atlantic is diminished under a warmer ocean climate. Global Change Biology 24:4386–4398.

Pfister, C. A., and M. A. Altabet. 2019. Enhanced microbial nitrogen transformations in association with macrobiota from the rocky intertidal. Biogeosciences 16:193–206.

Pfister, C. A., M. A. Altabet, S. Pather, and G. Dwyer. 2016. Tracer experiment and model evidence for macrofaunal shaping of microbial nitrogen functions along rocky shores. Biogeosciences 13:3519–3531.

Pfister, C. A., M. A. Altabet, and D. Post. 2014*a*. Animal regeneration and microbial retention of nitrogen along coastal rocky shores. Ecology 95:2803–2814.

Pfister, C. A., H. D. Berry, and T. Mumford. 2018. The dynamics of kelp forests in the northeast Pacific Ocean and the relationship with environmental drivers. Journal of Ecology 106:1520–1533.

Pfister, C. A., J. A. Gilbert, and S. M. Gibbons. 2014*b*. The role of macrobiota in structuring microbial communities along rocky shores. PeerJ 2:e631.

Reed, D. C., C. A. Carlson, E. R. Halewood, J. C. Nelson, S. L. Harrer, A. Rassweiler, and R. J. Miller. 2015. Patterns and controls of reef-scale production of dissolved organic carbon by giant kelp *Macrocystis pyrifera*: DOC production by giant kelp. Limnology and Oceanography 60: 1996–2008.

Reed, D. C., and M. S. Foster. 1984. The effects of canopy shadings on algal recruitment and growth in a giant kelp forest. Ecology 65:937–948.

Rosman, J. H., J. R. Koseff, S. G. Monismith, and J. Grover. 2007. A field investigation into the effects of a kelp forest (*Macrocystis pyrifera*) on coastal hydrodynamics and transport. Journal of Geophysical Research 112: C02016.

Stepien, C. C., C. A. Pfister, and J. T. Wootton. 2016. Functional traits for carbon access in macrophytes. PLoS ONE 11: e0159062.

Thompson, L. R. et al. 2017. A communal catalogue reveals Earth's multiscale microbial diversity. Nature 551:457–463.

UNESCO. 1994. Protocols for the joint global ocean flux study (JGOFS) core measurements. Volume 29. UNESCO-IOC, Paris, France.

Verges, A. et al. 2014. The tropicalization of temperate marine ecosystems: climate-mediated changes in herbivory and community phase shifts. Proceedings of the Royal Society B 281:20140846–20140846.

Vetter, E., and P. Dayton. 1999. Organic enrichment by macrophyte detritus, and abundance patterns of megafaunal populations in submarine canyons. Marine Ecology Progress Series 186:137–148.

Vollmers, J., M. Frentrup, P. Rast, C. Jogler, and A.-K. Kaster. 2017. Untangling genomes of novel planctomycetal and verrucomicrobial species from Monterey Bay kelp forest metagenomes by refined binning. Frontiers in Microbiology. https://doi.org/10.3389/fmicb.2017.00472

Wahl, M., S. Schneider Covachã, V. Saderne, C. Hiebenthal, J. D. Müller, C. Pansch, and Y. Sawall. 2018. Macroalgae may mitigate ocean acidification effects on mussel calcification by increasing pH and its fluctuations: biogenic fluctuations mitigate OA effects. Limnology and Oceanography 63:3–21.

Walters, W. et al. 2016. Improved bacterial 16S rRNA gene (V4 and V4–5) and fungal internal transcribed spacer marker gene primers for microbial community surveys. mSystems. https://doi.org/10.1128/msystems.00009-15

Webb, D. J., B. K. Burnison, A. M. Trimbee, and E. E. Prepas. 1992. Comparison of chlorophyll extractions with ethanol and dimethyl sulfoxide/acetone, and a concern about spectrophotometric phaeopigment correction. Canadian Journal of Fisheries and Aquatic Sciences 49:2331–2336.

Weigel, B. L., and C. A. Pfister. 2019. Successional dynamics and seascape-level patterns of microbial communities on the canopy-forming kelps *Nereocystis luetkeana* and *Macrocystis pyrifera*. Frontiers in Microbiology 10:346.

Welschmeyer, N. A., and C. J. Lorenzen. 1984. Carbon-14 labeling of phytoplankton carbon and chlorophyll *a* carbon: determination of specific growth rates: photosynthetic ^{14}C labeling. Limnology and Oceanography 29:135–145.

Wheeler, W. N., and L. D. Druehl. 1986. Seasonal growth and productivity of *Macrocystis integrifolia* in British Columbia, Canada. Marine Biology 90:181–186.

Wilmers, C. C., J. A. Estes, M. Edwards, K. L. Laidre, and B. Konar. 2012. Do trophic cascades affect the storage and flux of atmospheric carbon? An analysis of sea otters and kelp forests. Frontiers in Ecology and the Environment 10:409–415.

Wilson, J. M., S. Y. Litvin, and J. M. Beman. 2018. Microbial community networks associated with variations in community respiration rates during upwelling in nearshore Monterey Bay, California. Environmental Microbiology Reports 10: 272–282.

Wootton, J. T., and C. A. Pfister. 2012. Carbon system measurements and potential climatic drivers at a site of rapidly declining ocean pH. PLoS ONE 7:e53396.

Wootton, J. T., C. A. Pfister, and J. D. Forester. 2008. Dynamic patterns and ecological impacts of declining ocean pH in a high-resolution multi-year dataset. Proceedings of the National Academy of Sciences 105:18848–18853.

Yates, K. K., C. Dufore, N. Smiley, C. Jackson, and R. B. Halley. 2007. Diurnal variation of oxygen and carbonate system parameters in Tampa Bay and Florida Bay. Marine Chemistry 104:110–124.

Zhang, L., M. A. Altabet, T. Wu, and O. Hadas. 2007. Sensitive measurement of $NH_4^{+15}N/^{14}N$ ($\delta^{15}NH_4^+$) at natural abundance levels in fresh and saltwaters. Analytical Chemistry 79:5297–5303.

Supporting Information

Additional supporting information may be found in the online version of this article at http://onlinelibrary.wiley.com/doi/10.1002/ecy.2798/suppinfo